

In: *Computational Models of Molecular and Cellular Interactions*
(Edited by J. Bower and H. Bolouri)
Manuscript of July 21, 1998

**KINETIC MODELS OF MEMBRANE EXCITABILITY
AND SYNAPTIC INTERACTIONS**

Alain Destexhe

Laboratoire de Neurophysiologie
Département de Physiologie
Université Laval
Québec G1K 7P4, Canada

SUMMARY

This chapter reviews different approaches to model the ion channels underlying the electrical behavior of neurons in a way compatible with cellular biochemistry. Voltage-dependent channels, ligand-gated channels, and second-messenger-gated channels are modeled along the same lines. For each type of channel, different representations are considered, from biophysically detailed models to highly simplified two-state (open/closed) representations. These different kinetic models can be used according to the level of biophysical detail required, typically multistate Markov models are required to describe single-channel behavior while simplified models capture the most salient properties of synaptic interactions necessary for network simulations. The case of linking ion channel models with various intracellular processes is also considered. The dynamics of intracellular calcium, calcium-binding proteins, exocytosis and G-protein mediated responses can be integrated together with ion channels using similar kinetic equations. This allows to describe various processes such as electrical excitability, synaptic transmission and cellular biochemistry using the same formalism.

1 INTRODUCTION

Ion channels are transmembrane proteins containing a pore permeable specifically to one or several ionic species. This property of ionic selectivity is at the basis of the establishment of a voltage difference across the membrane (Hille, 1992). This membrane potential is influenced by opening or closing ion channels, and the control of the gating of ion channels by extracellularly released messenger molecules provides the basis for neuronal interactions. In addition, the permeability of some ion channels may depend on voltage. This property is fundamental to explain the electrical excitability of the membrane, as shown by the influential work of Hodgkin and Huxley (1952). Several types of voltage-dependent ion channels are present in central neurons and are responsible for a rich repertoire of electrical behavior essential for neuronal function (Llinás, 1988).

The biophysical properties of ion channels have been studied in depth using patch recording techniques (Sakmann and Neher, 1995). Single-channel recordings have shown that ion channels display rapid transitions between conducting and non-conducting states. It is now known that conformational changes of the channel protein give rise to opening/closing of the channel, as well as its voltage-sensitivity. Conformational changes can be described by state diagrams and Markov models analogous to conformational changes underlying the action of enzymes.

Markov models involving multiple conformational states are usually required to capture accurately the dynamics of single ion channels. However, this complexity may not be necessary in all cases and simpler models can be adequate to simulate larger scale systems. For example, networks of neurons in the central nervous system involve several types of neurons, each comprising multiple types of voltage-dependent ion channels, and the synaptic interactions are mediated by several types of synaptic receptors and their associated ion channels. Modeling such a system therefore requires to model thousands of ionic currents and representing each current by multistate Markov schemes is clearly not feasible with normal computing facilities.

In this chapter, we review kinetic models of ion channels, ranging from multistate Markov models to highly simplified schemes. We show that kinetic models can be used to describe a large spectrum of physiological processes involved in neuronal behavior, including voltage-dependent channels, synaptic transmission and second-messenger actions. We show that kinetic models provide a way to describe the electrical behavior of neurons by a unique formalism and that this formalism naturally connects to kinetic equations used to model biochemical reactions.

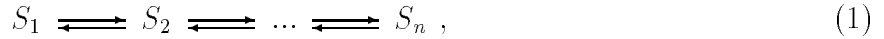
2 KINETIC MODELS OF ION CHANNELS

The molecular processes leading to opening and closing of ion channels may depend on various factors extrinsic to the channel, such as the electric field across the membrane or the binding of a ligand. The exact molecular mechanisms underlying the gating of ion channels are far from being understood (for a recent review, see Armstrong and Hille, 1998). Nevertheless, it is possible to describe the electrical properties of ion channels accurately (Hille, 1992). In this section, we review the general equations to describe the gating of ion channels and how to integrate them with membrane equations. Different classes of ion channels will be considered

in further sections.

2.1 The kinetic description of ion channel gating

Assuming that gating occurs following conformational changes of the ion channel protein, the sequence of conformations involved in this process can be described by state diagrams:



where $S_1 \dots S_n$ represents distinct conformational states of the ion channel. Define $P(S_i, t)$ as the probability of being in a state S_i at time t and $P(S_i \rightarrow S_j)$ as the *transition probability* from state S_i to state S_j :



The time evolution of the probability of state S_i is described by the *Master equation* (see e.g., Colquhoun and Hawkes, 1977, 1981):

$$\frac{dP(S_i, t)}{dt} = \sum_{j=1}^n P(S_j, t) P(S_j \rightarrow S_i) - \sum_{j=1}^n P(S_i, t) P(S_i \rightarrow S_j) . \quad (3)$$

The left term represents the “source” contribution of all transitions entering state S_i , and the right term represents the “sink” contribution of all transition leaving state S_i . In this equation, the time evolution depends only on the present state of the system, and is defined entirely by knowledge of the set of transition probabilities. Such systems are called *Markovian systems*.

In the limit of large numbers of identical channels or other proteins, the quantities given in the master equation can be replaced by their macroscopic interpretation. The probability of being in a state S_i becomes the *fraction of channels* in state S_i , noted s_i , and the transition probabilities from state S_i to state S_j become the *rate constants*, r_{ij} , of the reactions



In this case, one can rewrite the master equation as:

$$\frac{ds_i}{dt} = \sum_{j=1}^n s_j r_{ji} - \sum_{j=1}^n s_i r_{ij} \quad (5)$$

which is a conventional kinetic equation for the various states of the system.

Stochastic Markov models (as in Eq. 3) are adequate to describe ion channels as recorded using single-channel recording techniques (see Sakmann and Neher, 1995). In other cases, where a larger area of membrane is recorded and large numbers of ion channels are involved, the macroscopic currents are more adequately described by conventional kinetic equations (as in Eq. 5). In the following, only systems of the latter type will be considered.

2.2 Integration of kinetic models into neural models

Kinetic models of ion channels and other proteins are coupled through various types of interactions, which can be expressed by equations governing the electrical and chemical states of the cell.

Using the equivalent circuit approach, the general equation for the membrane potential of a single isopotential compartment is:

$$C_m \frac{dV}{dt} = \sum_{k=1}^n I_k , \quad (6)$$

where V is the membrane potential, C_m is capacitance of the membrane, and I_k are the contributions of all channels of one type to the current across a particular area of membrane. Only single compartments were simulated, but the same approach could be extended to multiple compartments using cable equations (Rall, 1995). In this case, a compartment may represent a small cylinder of dendritic or axonal process. We assumed that (a) the membrane compartment contained a sufficiently large number of channels of each type k for Eq. (5) to hold, and (b) there was a single open or conducting state, O_k , for each channel type with maximum single-channel conductance, γ_k . Then, to first approximation, each I_k can be calculated assuming a linear $I - V$ relationship, giving the familiar Ohmic form

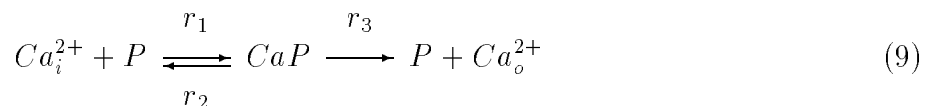
$$I_k = \bar{g}_k o_k (V - E_k) \quad (7)$$

where o_k is the fraction of open channels, \bar{g}_k is the maximum conductance and E_k is the equilibrium (reversal) potential. \bar{g}_k is the product of the single-channel conductance and the channel density, $\bar{g}_k = \gamma_k \rho_k$.

Calcium acts as ligand for many channels and proteins. In order to track the concentration of ions such this, standard chemical kinetics can also be used. The contribution of calcium channels to the free Ca^{2+} inside the cell was calculated as

$$\frac{d[\text{Ca}^{2+}]_i}{dt} = \frac{-I_{\text{Ca}}}{zFA d} \quad (8)$$

where $[\text{Ca}^{2+}]_i$ is the intracellular submembranal calcium concentration, $z = 2$ is the valence of Ca^{2+} , F is the Faraday constant, A is the membrane area, and $d = 0.1 \mu\text{m}$ is the depth of an imaginary submembrane shell. Removal of intracellular Ca^{2+} was driven by an active pump obeying Michaelis-Menten kinetics (see Destexhe et al., 1993a):



where P represents the Ca^{2+} pump, $\text{Ca}P$ is an intermediate state, Ca_o^{2+} is the extracellular Ca^{2+} and r_1 , r_2 , and r_3 are rate constants as indicated. Ca^{2+} ions have a high affinity for the pump P , whereas extrusion of Ca^{2+} follows a slower process (Blaustein, 1988). The extrusion process was assumed to be fast (milliseconds). Diffusion inside the cytoplasm was not included here but was considered in detail elsewhere in this volume (see Chapter ??).

3 VOLTAGE-DEPENDENT ION CHANNELS

Some ion channels may be gated by the electric field across the membrane. The opening of these channels may in turn influence the membrane potential. This interaction loop between membrane potential and ion permeability is at the basis of membrane excitability and the complex intrinsic firing properties of many neuron types. In this section, we describe different types of kinetic models to describe voltage-dependent channels and illustrate of these models compare to each other, using the generation of a classical sodium-potassium action potential as an example.

3.1 The kinetics of voltage-dependent gating

Voltage-dependent ion channels can be described using Markov kinetic schemes in which transition rates between some pairs of states, i and j , are dependent on the membrane potential, V :



According the theory of reaction rates (e.g., Johnson, Eyring and Stover, 1974), the rate of transition between two states depends exponentially on the free energy barrier between them:

$$r_{ij}(V) = \exp -U_{ij}(V)/RT, \quad (11)$$

where R is the gas constant and T is the absolute temperature. The free energy function $U_{ij}(V)$ is in general very difficult to evaluate, and may involve both linear and nonlinear components arising from interactions between the channel protein and the membrane electrical field. This dependence can be expressed without assumptions about underlying molecular mechanisms by a Taylor series expansion of the form

$$U(V) = c_0 + c_1V + c_2V^2 + \dots \quad (12)$$

giving a general transition rate function

$$r(V) = \exp[-(c_0 + c_1V + c_2V^2 + \dots)/RT], \quad (13)$$

where c_0 , c_1 , c_2 , ... are constants which are specific for each transition. The constant c_0 corresponds to energy differences that are independent of the applied field, the linear term c_1V to the translation of isolated charges or the rotation of rigid dipoles, and the higher order terms to effects such as electronic polarisation and pressure induced by V (Stevens, 1978; Andersen and Koeppe, 1992). In the ‘‘low field limit’’ (during relatively small applied voltages), the contribution of the higher order terms may be negligible (Stevens, 1978). Thus, a simple, commonly-used voltage dependence results from the first-order approximation of Eq. 13 and takes the form:

$$r_{ij}(V) = a_{ij} \exp(-V/b_{ij}), \quad (14)$$

where a_{ij} and b_{ij} are constants.

This simple exponential form for the voltage-dependence of rates constants is commonly used (eg, Chabala, 1984; Vandenberg and Bezanilla, 1991; Perozo and Bezanilla, 1990; Harris et al., 1981). However, the interactions of a channel protein with the membrane field might be expected to yield a rather more complex dependency (Stevens, 1978; Neher and Stevens, 1978; Andersen and Koeppe, 1992; Clay, 1989). Significantly, it has been shown that the number of states needed by a model to reproduce the voltage-dependent behavior of a channel may be reduced by adopting functions that saturate at extreme voltages (Keller et al., 1986; Clay, 1989; Chen and Hess, 1990; Borg-Graham, 1991). In this case, the following form can be used for voltage-dependent transition rates:

$$r_i(V) = \frac{a_i}{1 + \exp[-(V - c_i)/b_i]} \quad (15)$$

which can be obtained from Eq. (13) by considering nonlinear as well as linear components of the voltage dependence of the free energy barrier between states. The constant a_i sets the maximum transition rate, b_i sets the steepness of the voltage-dependence, and c_i sets the voltage at which the half-maximal rate is reached. Through explicit saturation, Eq. (15) effectively incorporates voltage-independent transitions that become rate-limiting at extreme voltage ranges (Keller et al. 1986, Vandenberg and Bezanilla, 1990, Chen and Hess, 1990), eliminating the need for additional closed or inactivated states (see discussion by Chen and Hess, 1990).

3.2 The Hodgkin-Huxley model of voltage-dependent channels

The most elementary Markov model for a voltage-gated channel is the first order scheme



with voltage-gated rates $r_1(V)$ and $r_2(V)$ between a single open or conducting state, O , and a single closed state C .

The model introduced by Hodgkin and Huxley (1952) described the permeability to Na^+ and K^+ ions in terms of gating particles described by open/closed transitions similar to Eq. 16. Interpreted in terms of ion channels, the Hodgkin-Huxley model considers that the channel is composed of several independent gates and that each gate must be in the open state in order the channel to conduct ions. Each gate has two states with first-order kinetics described by Eq. 16.

Gates are divided into two types, usually several gates for *activation*, m , and a single gate for *inactivation*, h . All activation gates are assumed to be identical to one another, reducing the number of state transitions that must be calculated to two

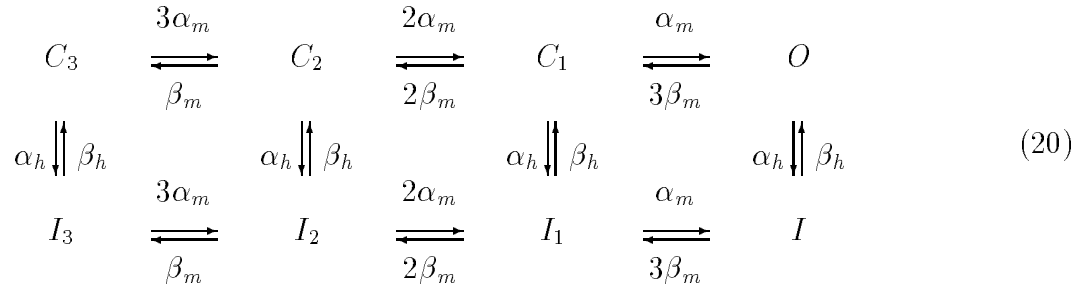


where C_m , O_m and C_h , O_h are the closed/open states of each m and h gates respectively. Because all gates must be open in order to allow the channel to conduct ions, the channel conductance is equal to the product of the fractions of gates in the open state, yielding

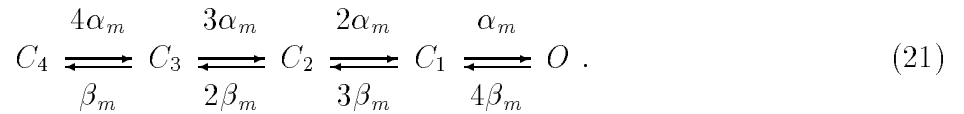
$$o = m^M h \quad (19)$$

where $m = [O_m]/[O_m + C_m]$, $h = [O_h]/[O_h + C_h]$, and M is the number of identical m gates.

The Hodgkin-Huxley formalism is a subclass of the more general Markov representation. An equivalent Markov model can be written for any Hodgkin-Huxley scheme, but the translation of a system with multiple independent particles into a single-particle description results in a combinatorial explosion of states. Thus, the Markov model corresponding to the Hodgkin-Huxley sodium channel is



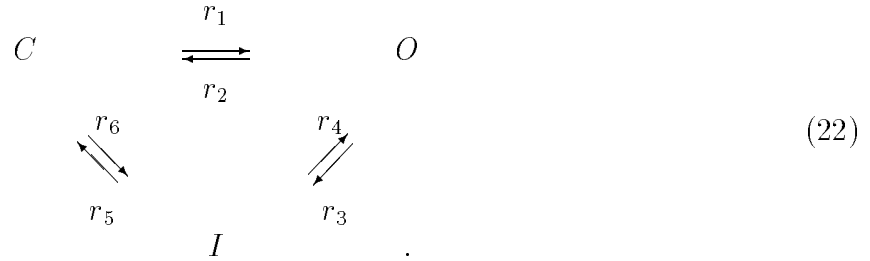
(FitzHugh, 1965). The states represent the channel with the inactivation gate in the open state (top) or closed state (bottom) and (from left to right) three, two, one or none of the activation gates closed. To reproduce the m^3 formulation, the rates must have the 3:2:1 ratio in the forward direction and the 1:2:3 ratio in the backward direction. Only the O state is conducting. The squid delayed rectifier potassium current modeled by Hodgkin and Huxley (1952) with 4 activation gates and no inactivation can be treated analogously (FitzHugh, 1965; Armstrong, 1969) giving



3.3 Markov models of voltage-dependent channels

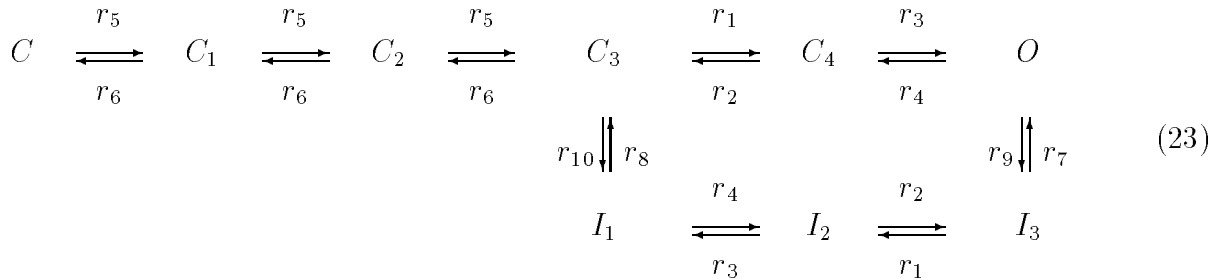
In more general models using Markov kinetics, independent and identical gates are not assumed. Rather, a state diagram is written to represent the set of configurations of the channel protein. This relaxes the constraints on the form of the diagram and the ratios of rate constants imposed by the Hodgkin-Huxley formulation. One may begin with the elementary two-state scheme

(Eq. 16) augmented by a single inactivated state, giving

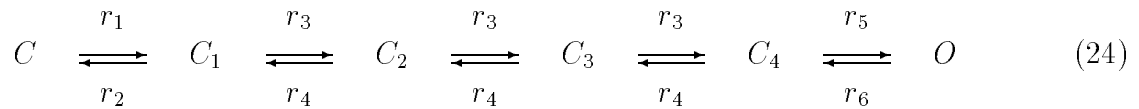


All six possible transitions between the three states are allowed, giving this kinetic scheme a looped form. The transition rates may follow voltage-dependent equations in the general form of Eq. (13) or some of these rates may be taken as either zero or independent of voltage to yield more simple models (see below).

To fit more accurately the time course of channel openings or gating currents, additional closed and inactivated states may be necessary. As an example of a biophysically-derived multistate Markov model, the squid sodium channel model of Vandenberg and Bezanilla (1991) was considered. The authors fit by least squares a combination of single channel, macroscopic ionic, and gating currents using a variety of Markov schemes. The nine state diagram



was found to be optimal by maximum likelihood criteria. The voltage-dependence of the transition rates was assumed to be a simple exponential function of voltage (Eq. 14). To complement the detailed sodium model of Vandenberg and Bezanilla, we also examined the six state scheme for the squid delayed rectifier used by Perozo and Bezanilla (1990)



where again rates were described by a simple exponential function of voltage (Eq. 14).

3.4 Example: models of voltage-dependent sodium currents

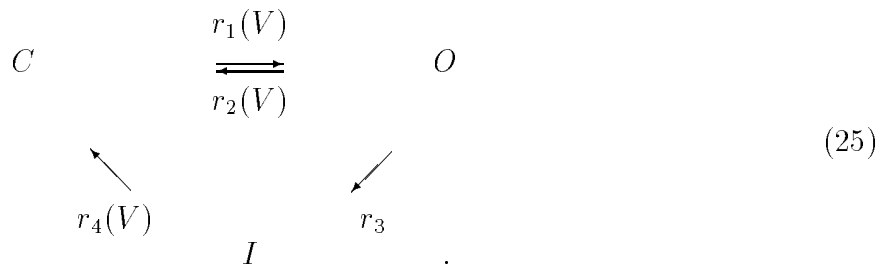
The different types of models reviewed above are characterized by different complexity, ranging from a two-state representation (Eq. 16) to transition diagrams involving many states (Eq. 23). The two-state description is adequate to fit the behavior of some channels (see eg, Labarca et al., 1980; Yamada et al., 1989; Borg-Graham, 1991; Destexhe et al., 1994b, 1994c, 1998b),

but for most channels more complex models must be considered. Many models of sufficient complexity are capable of fitting any limited set of experimental data. To demonstrate this, we compared three alternative models of the fast sodium channel underlying action potentials (Fig. 1).

First, the original quantitative description of the squid giant axon sodium conductance given by Hodgkin and Huxley (1952) was reproduced (Fig. 1A). The Hodgkin-Huxley (H-H) model had four independent gates each undergoing transitions between two states with first-order kinetics as described by Eqs. 17-18. Three identical m gates represent activation and one h gate for inactivation, leading to the familiar form for the conductance, $g_{Na} \propto m^3 h$ (Eq. 19).

Since the work of Hodgkin and Huxley, the behavior of the sodium channel of the squid axon has subsequently been better described in studies using Markov kinetic models. To illustrate the nature of these studies, we simulated the detailed sodium channel model of Vandenberg and Bezanilla (1991) (Eq. 23, Fig. 1B). This particular nine-state model was selected to fit not only the measurements of macroscopic ionic currents available to Hodgkin and Huxley, but also recordings of single channel events and measurements of currents resulting directly from the movement of charge during conformational changes of the protein (so-called *gating currents*).

We also used a simplified Markovian sodium channel model (Fig. 1C). The scheme was chosen to have the fewest possible number of states (three) and transitions (four) while still being capable of reproducing the essential behavior of the more complex models. The form of the state diagram was based on the looped three-state model (Eq. 22) with several transitions eliminated to give an irreversible loop (Bush and Sejnowski, 1991):



This model incorporated voltage-dependent opening, closing, and recovery from inactivation, while inactivation was voltage-independent. For simplicity, neither opening from the inactivated state nor inactivation from the closed state were permitted. Although there is clear evidence for occurrence of the latter (Horn et al., 1981) it was unnecessary under the conditions of our simulations. Rate constants were described by Eq. 15 with all $b_i = b$ and $c_1 = c_2$ to yield a model consisting of nine total parameters.

The response of the three sodium channel models to a voltage-clamp step from rest (-75 mV) was simulated (Fig. 1). For all three models, closed states were favored at hyperpolarized potentials. Upon depolarization, forward (opening) rates sharply increased while closing (backward) rates decreased, causing a migration of channels in the forward direction toward the open state. The three closed states in the Hodgkin-Huxley model and the five closed states in the detailed (Vandenberg-Bezanilla) model gave rise to the characteristic sigmoidal shape of the rising phase of the sodium current (Fig. 1D). In contrast, the simple model, with a single closed state, produced a first-order exponential response to the voltage step.

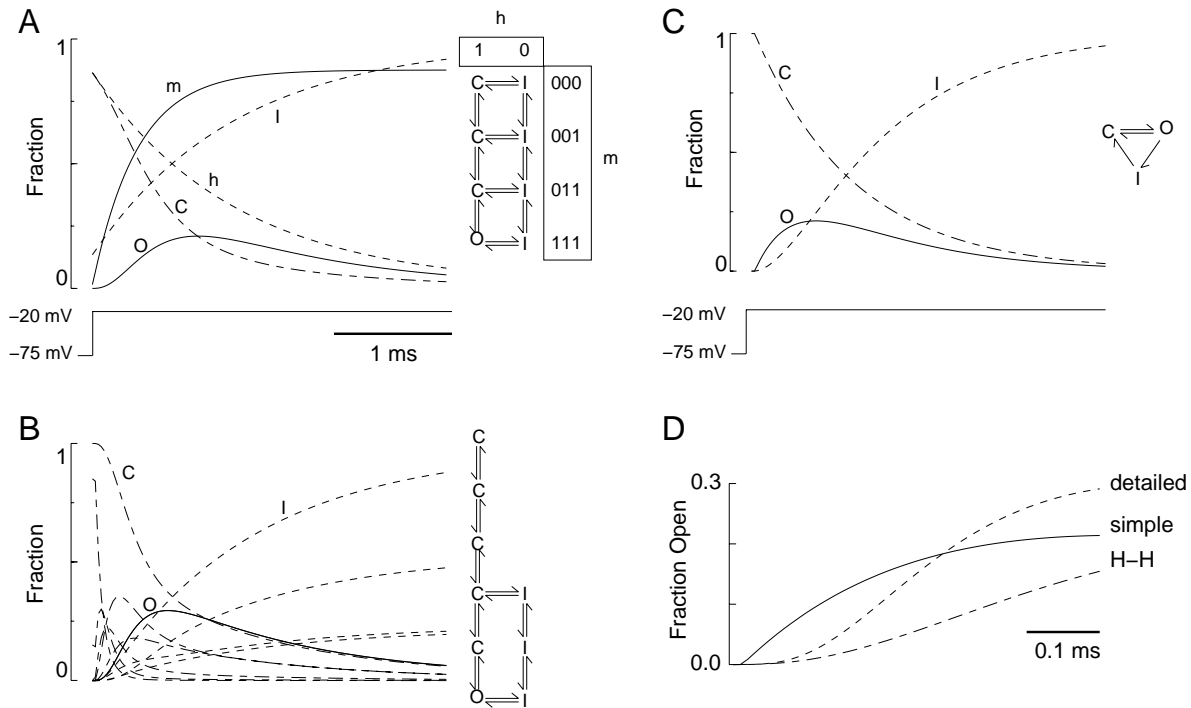


Figure 1:

Three kinetic models of a squid axon sodium channel produce qualitatively similar conductance time courses. A voltage-clamp step from rest, $V = -75 \text{ mV}$, to $V = -20 \text{ mV}$ was simulated. The fraction of channels in the open state (O , solid lines), closed states (C , dashed lines), and inactivated states (I , dotted lines) are shown for the Hodgkin-Huxley model, a detailed Markov model, and a simple Markov model. A. An equivalent Markov scheme for the Hodgkin-Huxley model is shown (right insert, Eq. 20). Three identical and independent activation gates (m , thin solid line) gives a form with 3 closed states (corresponding to 0, 1, and 2 activated gates) and one open state (3 activated gates). The independent inactivation gate, (h , thin dotted line) adds 4 corresponding inactivated states. Voltage-dependent transitions were calculated using the original equations and constants of Hodgkin and Huxley (1952). B. The detailed Markov model of Vandenberg and Bezanilla (1991) (Eq. 23). Individual closed and inactivated states are shown (thin lines) as well as the sum of all 5 closed and all 3 inactivated states (thick lines). C. A simple three-state Markov model fit to approximate the detailed model (Eq. 25). D. Comparison of the time course of open channels for the three models on a faster time scale shows differences immediately following a voltage step. The Hodgkin-Huxley model (dashed line) and detailed Markov modeled (solid line) give smooth, multiexponential rising phases, while the simple Markov model (dotted line) gives a single exponential rise with a discontinuity in the slope at the beginning of the pulse. Figure modified from Destexhe et al. (1994c) where all parameters are given.

Even though the steady-state behavior of the Hodgkin-Huxley model of the macroscopic sodium current is remarkably similar to that of the microscopic Markov models (Marom and Abbott, 1994), the relationship between activation and inactivation is different. First, in the Hodgkin-Huxley model, activation and inactivation are kinetically independent. This independence has been shown to be untenable on the basis of gating and ion current measurements in the squid giant axon (Armstrong, 1981; Bezanilla, 1985). Consequently, Markov models that are required to reproduce gating currents, such as the Vandenberg-Bezanilla model examined here, require schemes with coupled activation and inactivation. Likewise, in the simple model, activation and inactivation were strongly coupled due to the unidirectional looped scheme (Eq. 25), so that channels were required to open before inactivating and could not reopen from the inactivated state before closing.

Second, in the Hodgkin-Huxley and Vandenberg-Bezanilla models, inactivation rates are slow and activation rates fast. In simple Markov models, the situation was reversed, with fast inactivation and slow activation. At the macroscopic level modeled here, these two relationships gave rise to similar time course for open channels (Fig. 1A-C; see Andersen and Koeppe, 1992). However, the two classes of models make distinct predictions when interpreted at the microscopic (single-channel) level. Whereas the Hodgkin-Huxley and Vandenberg-Bezanilla models predict the latency to first channel opening to be short and channel open times to be comparable to the time course of the macroscopic current, the simplified Markov model predicts a large portion of first channel openings to occur after the peak of the macroscopic current and to have open times much shorter than its duration. Single channel recordings have confirmed the latter prediction (Sigworth and Neher, 1980; Aldrich et al., 1983; Aldrich and Stevens, 1987).

Despite the significant differences in their complexity and formulation, the three models of the sodium channel all produced very comparable action potentials and repetitive firing when combined with appropriate delayed-rectifier potassium channel models (Fig. 2). None of the potassium channel models had inactivation. The main difference was in the number of closed states, from six for the detailed Markov model of Perozo and Bezanilla (1990; Eq. 24), to four for the original (Hodgkin and Huxley, 1952) description of the potassium current, to just one for a minimal model (Eq. 16) with rates of sigmoidal voltage dependence (Eq. 15).

4 TRANSMITTER RELEASE

When action potentials reach the synaptic terminals of a neuron, they trigger the release of neurotransmitter in the extracellular space. Neurotransmitter molecules then bind to receptors and affect the voltage or the intracellular metabolism of the target cells. The release of transmitter involves complex calcium-dependent molecular mechanisms that links the arrival of an action potential in the synaptic terminal to the exocytosis of transmitter. This section makes the link between action potentials and transmitter release. Kinetic models incorporating various levels of detail are compared to simplified models of the release process.

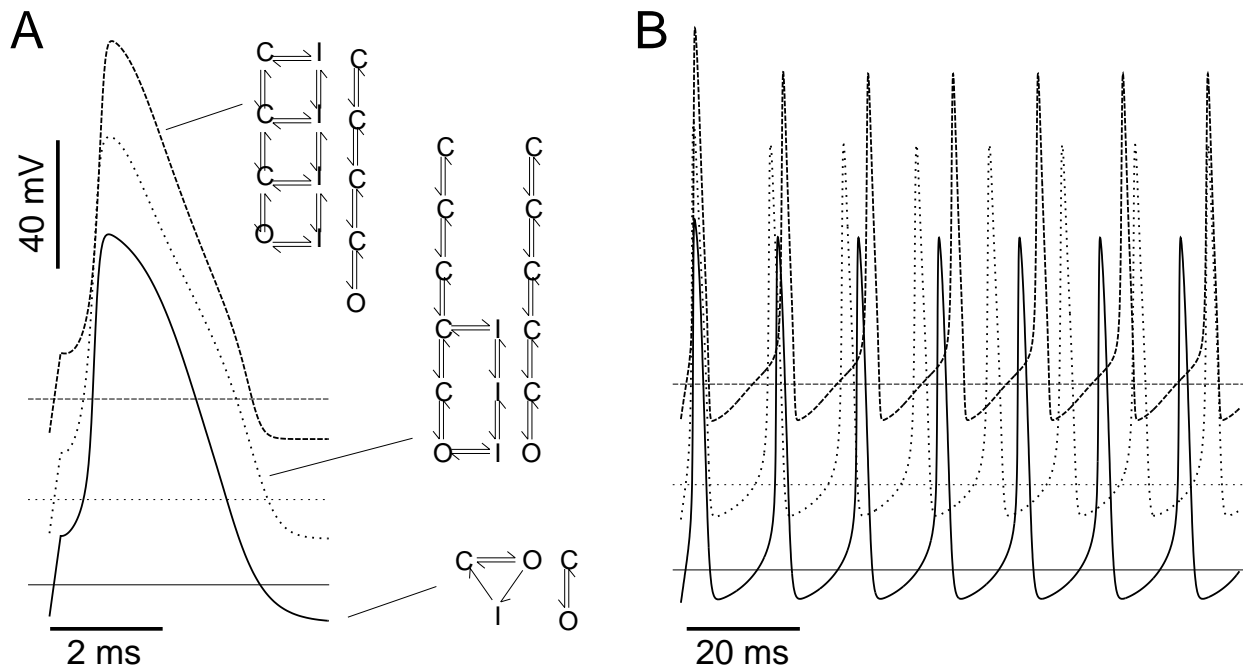


Figure 2:

Similar action potentials produced using three different kinetic models of squid fast sodium and delayed rectifying potassium channels. A. Single action potentials in response to 0.2 ms , 2 nA current pulse are elicited at similar thresholds and produce similar waveforms using three different pairs of kinetic models: Hodgkin-Huxley (dashed line; Hodgkin and Huxley, 1952), detailed Markov (dotted line; Vandenberg and Bezanilla, 1991; Perozo and Bezanilla, 1990), and 3-state Markov (solid line). B. Repetitive trains of action potentials elicited in response to sustained current injection (0.2 nA) have slightly different frequencies. Sodium channels were modeled as described in Fig. 1. The detailed Markov potassium channel model had 6 states (Perozo and Bezanilla, 1990) (Eq. 24) and the simple model of potassium channel had 2 states (Eq. 16). Figure modified from Destexhe et al. (1994c) where all parameters are given.

4.1 Kinetic model of transmitter release

The exact mechanisms whereby Ca^{2+} enters the presynaptic terminal, the specific proteins with which Ca^{2+} interacts, and the detailed mechanisms leading to exocytosis represent an active area of research (e.g., Neher, 1998). It is clear that an accurate model of these processes should include the particular clustering of calcium channels, calcium diffusion and gradients, all enzymatic reactions involved in exocytosis, and the particular properties of the diffusion of transmitter across the fusion pore and synaptic cleft. For our present purpose, we use a kinetic model of calcium-induced release inspired by Yamada and Zucker (1992). This model of transmitter release assumed that: (a) upon invasion by an action potential, Ca^{2+} enters the presynaptic terminal due to the presence of a high-threshold Ca^{2+} current; (b) Ca^{2+} activates a calcium-binding protein which promotes release by binding to the transmitter-containing vesicles; (c) an inexhaustible supply of “docked” vesicles are available in the presynaptic terminal, ready to release; (d) the binding of the activated calcium-binding protein to the docked vesicles leads to the release of n molecules of transmitter in the synaptic cleft. The latter process is modeled here as a first-order process with a stoichiometry coefficient of n (see details in Destexhe et al., 1994c).

The calcium-induced cascade leading to the release of transmitter was described by the following kinetic scheme:



Here, calcium ions bind to a calcium-binding protein, X , with a cooperativity factor of 4 (see Augustine and Charlton, 1986; and references therein), leading to an activated calcium-binding protein, X^* (Eq. 26). The associated forward and backward rate constants are k_b and k_u . X^* then reversibly binds to transmitter-containing vesicles, V_e , with corresponding rate constants k_1 and k_2 (Eq. 27). The exocytosis process is then modeled by an irreversible reaction (Eq. 28) where activated vesicles, V_e^* , release n molecules of transmitter, T , into the synaptic cleft with a rate constant k_3 . The values of the parameters of these reactions were based on previous models and measurements (Yamada and Zucker, 1992).

The concentration of the liberated transmitter in the synaptic cleft, $[T]$, was assumed to be uniform in the cleft and cleared by processes of diffusion outside the cleft (to the extrajunctional extracellular space), uptake or degradation. These contributions were modeled by a first-order

reaction (Eq. 29) where k_c is the rate constant for clearance of T . The values of parameters were detailed previously (Destexhe et al., 1994c).

Figure 3A shows a simulation of this model of transmitter release associated to a single compartment presynaptic terminal containing mechanisms for action potentials, high-threshold calcium currents and calcium dynamics (see Destexhe et al., 1994c for details). Injection of a short current pulse into the presynaptic terminal elicited a single action potential. The depolarization of the action potential activated high-threshold calcium channels, producing a rapid influx of calcium. The elevation of intracellular $[Ca^{2+}]$ was transient due to clearance by an active pump. The time-course of activated calcium-binding proteins and vesicles followed closely the time-course of the transient calcium rise in the presynaptic terminal. This resulted in a brief (≈ 1 ms) rise in transmitter concentration the synaptic cleft (Fig. 3A, bottom curve D). The rate of transmitter clearance was adjusted to match the time course of transmitter release estimated from patch clamp experiments (Clements et al., 1992; Clements, 1996) as well as for detailed simulations of extracellular diffusion of transmitter (Bartol et al., 1991; Destexhe and Sejnowski, 1995).

4.2 Simplified models of the release process

The above-described release model would be computationally very expensive if it had to be used in network simulations involving thousands of synapses. Therefore, for large-scale network models, simplification of the release process is needed. The first alternative is to use a continuous function to transform the presynaptic voltage into transmitter concentration. An expression for such a function was derived previously (Destexhe et al., 1994c) by assuming that all intervening reactions in the release process are relatively fast and can be considered at steady state. The stationary relationship between the transmitter concentration $[T]$ and presynaptic voltage was well fit by the following relation (Destexhe et al., 1994c):

$$[T] = \frac{T_{max}}{1 + \exp[-(V_{pre} - V_p)/K_p]} \quad (30)$$

where T_{max} is the maximal concentration of transmitter in the synaptic cleft, V_{pre} is the presynaptic voltage, $K_p = 5$ mV gives the steepness and $V_p = 2$ mV sets the value at which the function is half-activated. One of the main advantages of using Eq. 30 is that it provides a very simple and smooth transformation between presynaptic voltage and transmitter concentration. Using this direct function provides a fair approximation of the transmitter concentration (Fig. 3B). This form, in conjunction with simple kinetic models of postsynaptic channels, provides a model of synaptic interaction based on autonomous differential equations with only one or two variables (see also Wang and Rinzel, 1992).

The second alternative is to assume that the change in the transmitter concentration occurs as a brief pulse (Destexhe et al., 1994b). There are many indications that the exact time course of transmitter in the synaptic cleft is not, under physiological conditions, a main determinant of the time course of postsynaptic responses at many synapses (eg Magleby and Stevens, 1972; Lester et al., 1990; Colquhoun et al., 1992; Clements et al., 1992). Indeed, fast application techniques have shown that 1 ms pulses of 1 mM glutamate reproduced PSCs in membrane

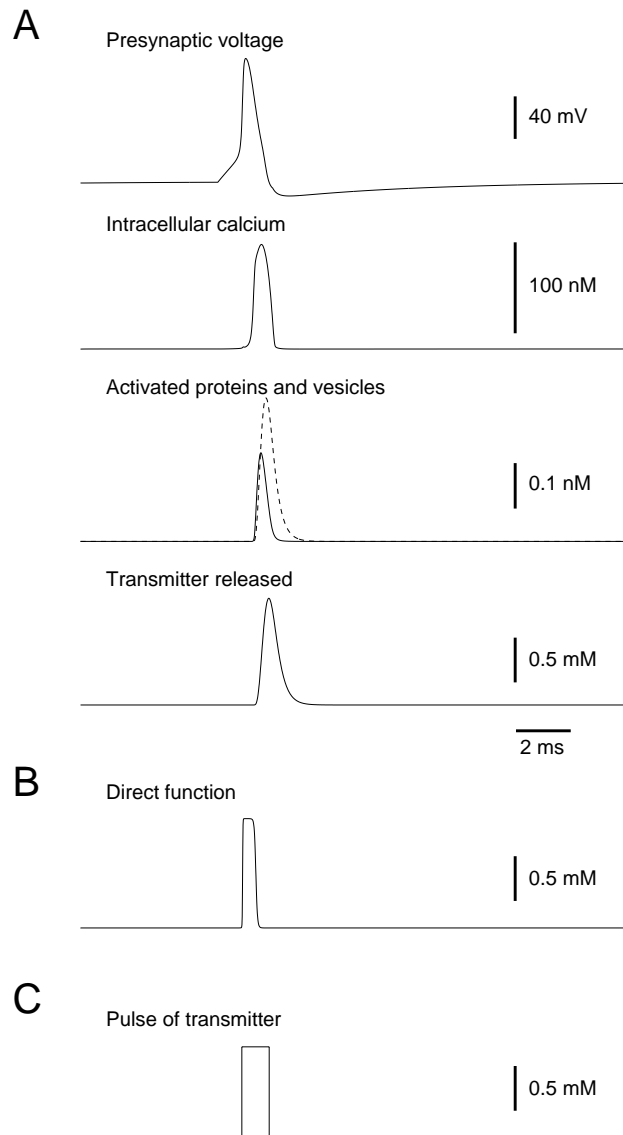


Figure 3:

Models of synaptic release. A. Kinetic model of presynaptic reactions leading to transmitter release. A presynaptic action potential elicited by injection of a 0.1 nA current pulse lasting 2 ms in the presynaptic terminal (top curve). The intracellular Ca^{2+} concentration in the presynaptic terminal increased (second curve) due to the presence of a high-threshold calcium current that provided a transient calcium influx during the action potential. Removal was provided by an active calcium pump. The relative concentration of activated calcium-binding protein X^* (third curve; solid line) and vesicles V_e^* (third curve; dotted line) also increased transiently, as did the concentration of transmitter in the synaptic cleft (bottom curve). B. Approximation of the transmitter time course using a direct sigmoid function of the presynaptic voltage. C. Pulse of 1 ms and 1 mM shown for comparison. Panel A was modified from Destexhe et al. (1994c) where all parameters were given.

patches that were quite similar as those recorded in the intact synapse (Hestrin 1992; Colquhoun et al., 1992; Sakmann and Neher, 1995; Standley et al., 1993). A pulse of 1 ms and 1 mM is shown in Fig. 3C and provides the simplest approximation of the time course of transmitter.

In models, using either release simulated by a kinetic model or simulated by a pulse of transmitter had barely detectable influence on the time course of the synaptic current (see Destexhe et al., 1994c, 1998b). Interestingly, pulse-based Markov models can be solved analytically, leading to very fast algorithms to simulate synaptic currents (Destexhe et al., 1994b, 1994c, 1998b). Pulse-based models are considered in the next Section.

5 LIGAND-GATED SYNAPTIC ION CHANNELS

An important class of ion channels remain closed until a ligand binds to the channel, inducing a conformational change allowing channel opening. This class of gating properties is referred as *ligand-gating*. A principle class of ligand-gated channels is those activated directly by neurotransmitter. In this case, the receptor and the ion channel are part of the same protein complex, which is called *ionotropic receptor*. Ligand gating also commonly occurs through secondary agonists, such as the glycine activation of the glutamate N-methyl-D-aspartate (NMDA) receptor, or through second-messengers, such as calcium, G-proteins, or cyclic nucleotides. In this section, we review different kinetic models for synaptic ion channels gated by neurotransmitter molecules. We illustrate the behavior of these models using fast glutamate-mediated neurotransmission as an example.

5.1 Kinetic models of ligand-gated channels

In general, for a ligand-gated channel, transitions rates between an unbound and bound states of the channel depends on the binding of a ligand:



where T is the ligand, S_i is the unbound state, S_j is the bound state (sometimes written $S_i T$), r_{ij} and r_{ji} are rate constants as defined before.

The same reaction can be rewritten as:



where $r_{ij}([T]) = [T] r_{ij}$ and $[T]$ is the concentration of ligand. Written in this form, Eq. 32 is equivalent to Eq. 10. Ligand-gating schemes are generally equivalent to voltage-gating schemes, although the functional dependence of the rate on $[T]$ is simple compared to the voltage-dependence discussed before.

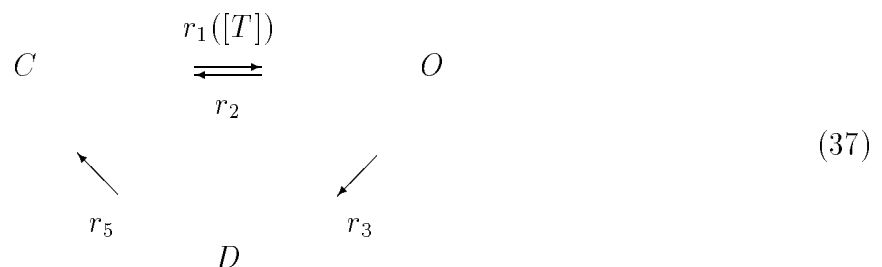
where C is the unbound closed state, C_1 and C_2 are respectively the singly- and doubly-bound closed states, O is the open state, and D_1 and D_2 are respectively the desensitized singly- and doubly-bound states.

Markov models were proposed for various other receptor types, including NMDA or γ -aminobutyric acid (GABA) type A receptors (reviewed in Sakmann and Neher, 1995). For ionotropic receptor types, detailed Markov models as well as simplified kinetic models consisting of fewer states have been proposed and compared (Destexhe et al., 1994c, 1998b). We illustrate this approach below by considering the example of AMPA receptors.

5.3 Example: glutamate AMPA receptors

Glutamate AMPA receptors are used here to compare the behavior of different models of ligand-gated receptors. The behavior of the detailed, six-state model for AMPA receptors derived by Standley et al. (1993; Eq. 36) is illustrated in Fig. 4A in conjunction with the detailed model of transmitter release described before. The postsynaptic response showed a fast time to peak of about 1 *ms* and a decay phase lasting 5 – 10 *ms*, in agreement with Standley et al. (1993). In addition, the response to a series of presynaptic action potentials at a rate of approximately 20*Hz* shows a progressive desensitization of the response due to the increase of the fraction of desensitized channels (states D_1 and D_2). A similar behavior was also found with another model of the AMPA current (Raman and Trussell, 1992; not shown).

Simplified models were obtained by using pulses of transmitter and fewer states in the Markov scheme. Using pulse of transmitters is justified by fast-perfusion experiments showing that 1 *ms* pulses of glutamate applied to patches containing AMPA receptors produced responses that closely matched the time course of synaptic currents (Colquhoun et al., 1992; Hestrin, 1992). The simplified diagram was found by comparing all possible two- and three-state schemes to the detailed model. The following three-state model



was found to be the best approximation for AMPA current (Destexhe et al., 1994c). Here, D represents the desensitized state of the channel and $r_1 \dots r_5$ are the associated rate constants. The time course of PSCs simulated by this model reproduced the progressive desensitizing responses (Fig. 4B) as well as the time course of the AMPA current observed in the more accurate model. On the other hand, simpler two-state models (Eq. 33) provided good fits of single PSCs, but did not account for desensitization (Destexhe et al., 1994c).

These models were compared to the *alpha function*, originally introduced by Rall (1967):

$$r(t - t_0) = \frac{(t - t_0)}{\tau_1} \exp[-(t - t_0)/\tau_1]. \tag{38}$$

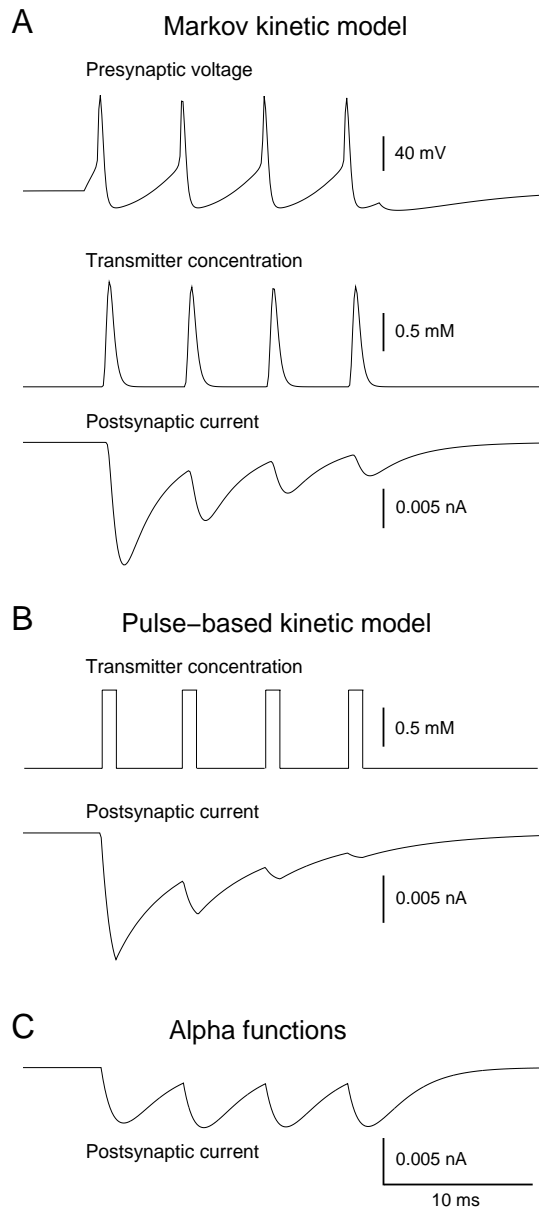


Figure 4:

Comparison of three models for AMPA receptors. A. Markov model of AMPA receptors. A presynaptic train of action potentials was elicited by current injection (Presynaptic voltage). The release of glutamate was calculated using a kinetic model of synaptic release (transmitter concentration). The postsynaptic current from AMPA receptors was modeled by a six-state Markov model. B. Same simulation with transmitter modeled by pulses (transmitter concentration) and AMPA receptors modeled by a simpler three-state kinetic scheme (postsynaptic current). C. Postsynaptic current modeled by summed alpha functions. Modified from Destexhe et al. (1994c).

This function gives a stereotyped waveform for the time course of the postsynaptic current following a presynaptic spike occurring at time $t = t_0$. τ_1 is the time constant of the alpha function. Alpha functions often provide approximate fits for many synaptic currents, and have been widely used for computing synaptic currents in neural models (see e.g., Koch and Segev, 1998).

The summation behavior of alpha functions is illustrated in Fig. 4C. In this case, there was no desensitization, and the fit of alpha functions to the the time course of the AMPA PSCs was poor (the rise time was too slow compared to the decay time).

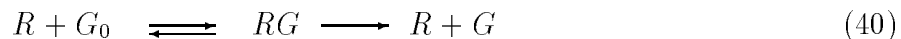
6 SECOND-MESSENGER-GATED SYNAPTIC CHANNELS

By contrast to ionotropic receptors, for which the receptor and ion channel are both part of the same protein complex, other classes of synaptic responses are mediated by an ion channel that is independent of the receptor. In this case, the binding of the neurotransmitter to the receptor induces the formation of an intracellular second-messenger, which in turn activates (or inactivates) ion channels. The advantage of this type of neurotransmission is that a single activated receptor can lead to the formation of thousands of second-messenger molecules, therefore providing an efficient amplification mechanism.

These so-called *metabotropic* receptors not only act on ion channels but may also influence several key metabolic pathways in the cell through second-messengers such as G-proteins or cyclic nucleotides. In this section, we review kinetic models for synaptic interactions acting through second-messengers. We illustrate this type of interactions using the example of GABA_B receptors, whose response is mediated by K⁺ channels through the activation of G-proteins (Andrade et al., 1986).

6.1 Kinetic models of second-messenger-gated channels

One particularity of metabotropic responses is that the receptor is part of a protein complex that also catalyzes the production of an intracellular second-messenger. These steps can be represented by the general scheme:

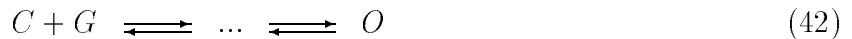


Here, the transmitter, T , binds to the receptor, R_0 , leading to its activated form, R , and desensitized form, D (Eq. 39). The activated receptor R catalyzes the formation of an intracellular second-messenger, G , from its inactive form, G_0 , through a Michaelis-Menten scheme (Eq. 40). Finally, the second-messenger is degraded back into its inactive form (Eq. 41).

The intracellular messenger G can affect various ion channels as well as the metabolism of the cell. The second-messenger may act directly on its effector, as demonstrated for some K⁺ channels that are directly gated by G-proteins (VanDongen et al., 1988). However, more

complex reactions may be also be involved, as in the case of phototransduction (see Lamb and Pugh, 1992).

We consider the simplest case of direct binding of the second-messenger to the ion channel, leading to its activation:



or de-activation:

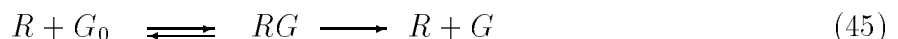


The first case (Eq. 42) is analogous to ligand-gated channels, the channel opens following the binding of one or several molecules of second-messenger. In the second case (Eq. 43), the channel is open at rest but closes following the binding of G . These types of gating may be characterized by Markov schemes involving several states, analogously to schemes considered for ionotropic receptors in Section 5.

Neurotransmitters including glutamate (through metabotropic receptors), GABA (through GABA_B receptors), acetylcholine (through muscarinic receptors), noradrenaline, serotonin, dopamine, histamine, opioids, and others, have been shown to mediate slow intracellular responses. These neurotransmitters induce the intracellular activation of G proteins, which may affect ionic currents as well as the metabolism of the cell. One of the main electrophysiological target of many neuromodulators is to open or close K⁺ channels (see Brown, 1990; Brown and Birnbaumer, 1990; McCormick, 1992). This type of action is illustrated below for GABA acting on GABA_B receptors.

6.2 Example: GABA_B-mediated neurotransmission

GABA_B receptors mediate slow inhibitory responses mediated by K⁺ channels through the activation of G-proteins (Andrade et al., 1986; Dutar and Nicoll, 1988). There is strong evidence that direct G-protein binding mediates the gating process (Andrade et al., 1986; Thalmann, 1988; Brown and Birnbaumer, 1990). The typical properties of GABA_B-mediated responses in hippocampal and thalamic neurons can be reproduced assuming that several G-proteins directly bind to the associated K⁺ channels (Destexhe and Sejnowski, 1995), leading to the following scheme:



where symbols have the same meaning as above and n is the number of independent binding sites of G-proteins on K⁺ channels.

The current is then given by:

$$I_{GABA_B} = \bar{g}_{GABA_B} [O] (V - E_K)$$

where $[O]$ is the fraction of K^+ channels in the open state.

The behavior of this model is shown in Fig. 5. Very brief changes in transmitter concentration gave rise to a much longer duration intracellular response. The rate constants of enzymatic reactions were estimated based on pharmacological manipulations and recordings *in vivo* (Breitwieser and Szabo, 1988; Szabo and Otero, 1989). In this simulation, the release was obtained according to the kinetic model of synaptic release and the K^+ channel was gated by G according to a simple two-state scheme involving 4 binding sites for G . Based on whole-cell recordings of $GABA_B$ currents in dentate granule cells (Otis et al., 1993), the rate constants of this model were adjusted to experimental data using a simplex fitting procedure (Destexhe and Sejnowski, 1995; Destexhe et al., 1998b).

This model reproduces a nonlinear dependence of $GABA_B$ responses to the number of presynaptic spikes. A single presynaptic action potential induces a relatively small increase of G-protein, which is insufficient to activate significant postsynaptic response (Fig. 5, dashed lines). However, a train of 10 presynaptic spikes at high frequency induces higher levels of activated G-proteins and evokes a significant postsynaptic response (Fig. 5, continuous lines). This type of dependence explains experimental observations that $GABA_B$ responses only appear under high stimulus intensities (Dutar and Nicoll, 1988; Kim et al., 1997) and the absence of $GABA_B$ -mediated miniature events (Thompson and Gähwiler, 1992; Otis and Mody, 1992).

A simplified two-state model of $GABA_B$ -mediated responses must include the sensitivity to the number of spikes. A one-variable model (corresponding to an open/closed scheme) would be too simple in this case. The simplest two-variable model was obtained from the model above, by considering Eq. 45 and Eq. 47 at steady-state, by considering G_0 in excess, and by neglecting $GABA_B$ receptor desensitization. This simplified two-variable model of $GABA_B$ -mediated currents was (Destexhe et al., 1998b):

$$\frac{dr}{dt} = K_1 T (1 - r) - K_2 r \quad (48)$$

$$\frac{dg}{dt} = K_3 r - K_4 g \quad (49)$$

where r is the fraction of receptors in the active form, T is the GABA concentration in the synaptic cleft, and g is the normalized concentration of G-proteins in the active state. The current is then given by:

$$I_{GABA_B} = \bar{g}_{GABA_B} \frac{g^n}{g^n + K_d} (V - E_K) \quad (50)$$

where \bar{g}_{GABA_B} is the maximal conductance of K^+ channels, E_K is the potassium reversal potential, and K_d is the dissociation constant of the binding of G-proteins on K^+ channels. These parameters were estimated by fitting the model to experimental data using a simplex procedure (see Destexhe et al., 1998b).

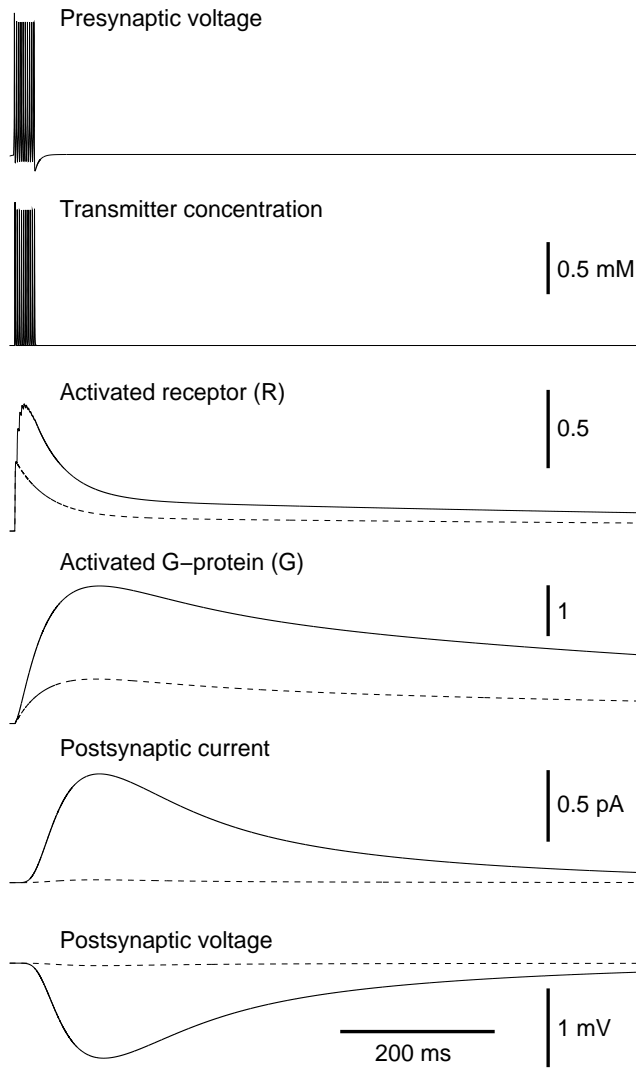


Figure 5:

Model of synaptic interactions mediated by second-messengers. The model simulates slow inhibitory responses mediated by $GABA_B$ receptors through the activation of G-proteins. The response is shown following a presynaptic train of 10 action potentials at high frequency (~ 300 Hz). The transmitter concentration was calculated using the kinetic model of release shown in Fig. 3A. The fraction of activated receptor (R) and G-protein (G), as well as the postsynaptic current and voltage are shown. Very brief synaptic events can evoke slow intracellular changes through the production of second-messengers (G-proteins here). The response to a train of 10 presynaptic spikes (continuous lines) is compared to that of a single presynaptic spike (dashed lines).

The behavior of the simplified model is shown in Fig. 6. Transmitter concentration was described by pulses of transmitter, as shown above and provided similar time course and stimulus dependence as the detailed model. A single presynaptic action potential induced low intracellular levels of activated G-protein, which were insufficient to evoke a postsynaptic response (Fig. 6, dashed lines). However, a train of 10 presynaptic spikes at ~ 300 Hz induced G-protein concentrations that were high enough to activate a postsynaptic response (Fig. 6, continuous lines), similarly to the detailed model (compare with Fig. 5).

7 APPLICATIONS TO MODEL COMPLEX NEURONAL INTERACTIONS

Modeling ion channels and synaptic interactions with the appropriate formalism is required in problems where the kinetics of ions channels are important. The case of the thalamus is a good example: thalamic neurons have complex intrinsic firing properties due to the presence of several types of voltage-dependent currents (Steriade and Llinás, 1988) and synaptic connections between thalamic cells are mediated by different types of ionotropic and metabotropic receptors (McCormick, 1992). Moreover, thalamic neurons and interconnectivity patterns have been well characterized by anatomists (Jones, 1985) and the thalamus exhibits pronounced oscillatory properties which have been well characterized *in vivo* and *in vitro* (see Steriade et al., 1993). Despite the abundant anatomical and physiological information available for this system, the exact mechanisms leading to oscillatory behavior are still open because of the complexity of the interactions involved.

Thalamic oscillations have been explored by computational models (Andersen and Rutjord, 1964; Destexhe et al., 1993b; Wang et al., 1995; Destexhe et al., 1996a; Golomb et al., 1996; reviewed in Destexhe and Sejnowski, 1997). At the single-cell level, models investigated the ionic mechanisms underlying the repertoire of firing properties of thalamic neurons based on voltage-clamp data on the voltage- and calcium-dependent currents present in these cells (McCormick and Huguenard, 1992; Destexhe et al., 1993a, 1996b). At the network level, synaptic interactions were simulated using the main receptor types identified in thalamic circuits (Destexhe et al., 1993b; Wang et al., 1995; Destexhe et al., 1996a; Golomb et al., 1996). Circuits of thalamic neurons were found to exhibit oscillatory behavior due to the interaction between inhibition and the bursting properties of thalamic neurons (Fig. 7). Simulating circuits of thalamic neurons interconnected with glutamatergic and GABAergic receptors produced oscillations that matched experimental observations if intrinsic and synaptic currents had kinetics compatible with voltage-clamp experiments (Destexhe et al., 1996a).

Experiments in thalamic slices (vonKrosigk et al., 1993) demonstrated that in the same circuit, the 8-12 Hz spindle oscillations can be transformed into a slower (2-4 Hz) and more synchronized oscillation following addition of bicuculline, a GABA_A receptor antagonist. Models could account for these observations only if GABA_B receptors had a nonlinear dependence on the number of presynaptic spikes (see Section 6). This transformation is shown in Fig. 7B-C. These models of small circuits were also extended to larger networks of thalamic neurons and the propagating properties found in ferret thalamic slices (Kim et al., 1995) could be reproduced by

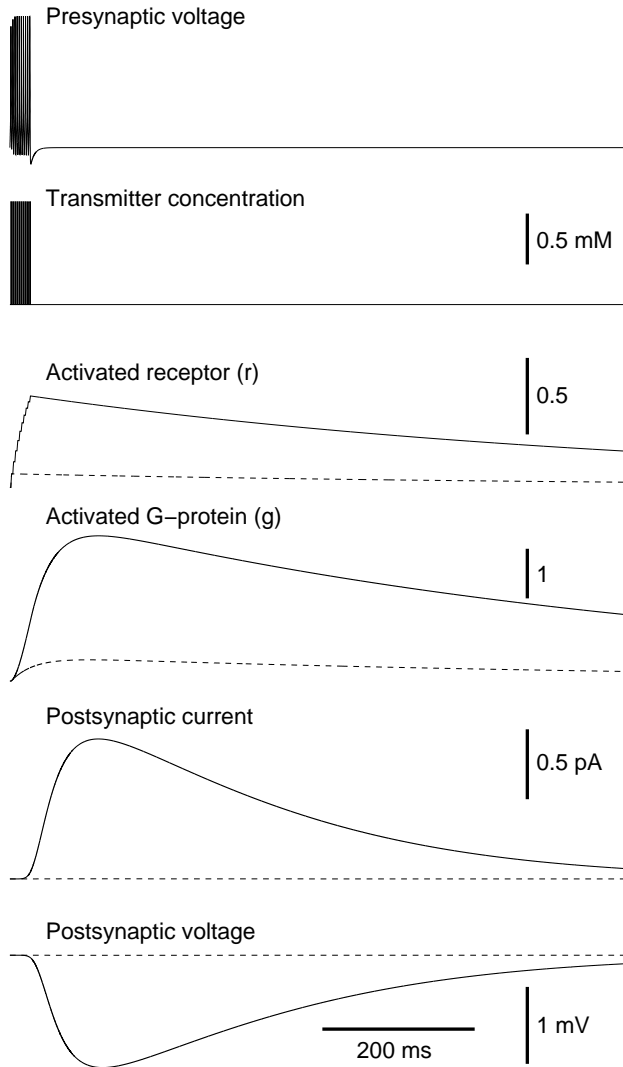


Figure 6:

Simplified model of $GABA_B$ -mediated responses. The same paradigm as in Fig. 5 is shown here using the simplified model. Presynaptic trains of action potentials were the same as in Fig. 5. Transmitter concentration was described by brief pulses (1 ms) and the fraction of activated receptor (r) and G-protein (g), as well as the postsynaptic current and voltage are shown for the simplified two-variable model (Eqs. 49). The response to trains of 10 presynaptic spikes (continuous lines) or to single presynaptic spike (dashed lines) are similar to the detailed model (compare with Fig. 5).

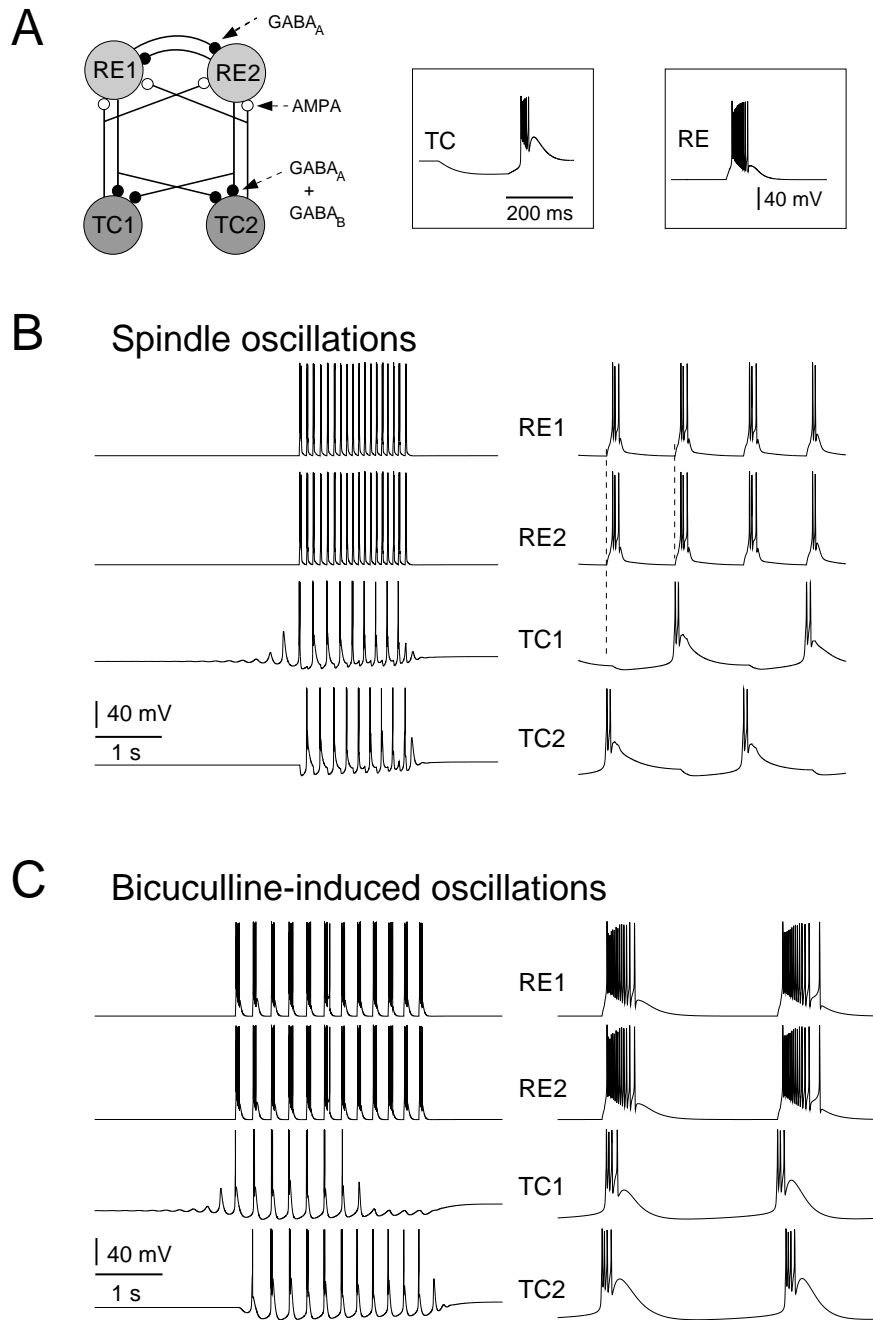


Figure 7:

Modeling the interplay of intrinsic and synaptic currents in networks of thalamic neurons. A. Scheme of a circuit of thalamic cells. Thalamocortical relay (TC) and thalamic reticular (RE) neurons are connected with AMPA, $GABA_A$ and $GABA_B$ receptors. Each cell type also generates bursts of action potentials in response to current injection (insets) due to the presence of a low-threshold calcium current. B. 8-12 Hz spindle oscillations arising from the mutual excitatory and inhibitory loop between TC and RE cells. In this case, RE cells produce few action potentials and the IPSP in TC cells is dominated by $GABA_A$ -mediated currents. TC cells fire every 2 cycles in alternation (left panel). C. 2-4 Hz oscillations obtained when $GABA_A$ receptors are suppressed. In this case, all cells oscillate in phase (left panel) and the large bursts produced by RE cells evoke $GABA_B$ -mediated IPSPs in TC cells. Modeling the phase relations and the coexistence of these two types of oscillations requires to model intrinsic and synaptic currents with correct kinetics and the nonlinear dependence of $GABA_B$ responses (modified from Destexhe et al., 1996a).

the model (Destexhe et al., 1996a). Similar conclusions were also reached by another modeling investigation (Golomb et al., 1996).

Models based on accurate kinetic representations of intrinsic and synaptic currents therefore reproduce experimental data, both at the single-cell level, for the repertoire of firing properties of thalamic cells, and at the network level, for the genesis of oscillations and their spatiotemporal properties. Models were also used to investigate hypotheses, such as why the reticular nucleus oscillates *in vivo* but not *in vitro* (Destexhe et al., 1994a). Models were also used to investigate mechanisms of synchronization in more complex thalamocortical networks and proposed a possible mechanism that explains apparently conflicting experimental observations from *in vitro* (Kim et al., 1995) and *in vivo* recordings (Contreras et al., 1996, 1997), as well as provided predictions to test this mechanism (see Destexhe et al., 1998a).

In conclusion, this example shows that simplified kinetic models are useful tools to study network mechanisms involving large numbers of neurons and synapses. Using Hodgkin-Huxley type models for representing voltage-dependent currents and simplified kinetic models for representing synaptic currents led to population behavior consistent with experimental measurements. To yield correct oscillation frequency and phase relations, the modeled ionic currents had to have rise/decay kinetics consistent with experimental data, but other properties were not required, such as AMPA receptor desensitization or the activation-inactivation coupling in sodium channels. This suggests that the rise/decay kinetics of currents are important determinants for this type of network behavior.

8 DISCUSSION

This chapter reviewed kinetic models for ion channels underlying membrane excitability, synaptic transmission and second-messenger actions. We discuss here the assumptions and limits of kinetic models and how to include these in a more general framework including the metabolism of the cell.

8.1 Assumptions of kinetic models

Markov kinetic models assume that (a) the gating of ion channels can be described by transition diagrams involving a finite number of states; (b) the transition probability between these states is independent of time. Because the flux of ions through single channels can be directly measured, it has been possible to observe directly the rapid and stochastic transitions between conducting and non-conducting states (Neher and Sakmann, 1976). Such rapid transitions are predicted by finite-state diagrams by opposition to a continuum of states which would predict smooth variations of current. A finite number of states is also justified thermodynamically by the existence of local energy minimas, with the consequence that the configuration of the channel protein in the membrane can be approximated by a set of distinct conformational states separated by large energy barriers (Hille, 1992).

Several alternative formalism have been suggested to model ion channels. Diffusional (Millhauser et al., 1988) or continuum gating models (Levitt, 1989), are Markovian but posit an

infinite number of states. Fractal (Liebovitch and Sullivan, 1987), or deterministically chaotic (Liebovitch and Toth, 1991) models assume a finite number of states, but allow time-dependent transition rates. Differentiation between discrete multistate Markov models and any of these alternatives hinges on high time-resolution studies of channel openings. Analysis of single-channel openings and closings has shown that finite-state Markov models are most consistent with experimental data (McManus et al., 1988; Sansom et al., 1989). Moreover, finite-state Markov models have been so far successful to account for nearly all types of ion channels recorded with single-channel techniques (see Hille, 1992; Sakmann and Neher, 1995).

8.2 Simplified models

Although a substantial number of states are necessary to account for the single-channel and macroscopic behavior of ion channels, this complexity is not always necessary. The voltage-dependent sodium channel was shown to be best described by a Markov model involving nine states (Vandenberg and Bezanilla, 1991) but the simpler model of Hodgkin and Huxley (1952), as well as simplified three-state models (Destexhe et al., 1994c), generated similar action potentials (Fig. 2). For synaptic ion channels, the phenomenon of receptor desensitization can be modeled relatively well using a three-state scheme (Fig. 4). Therefore, models incorporating different levels of complexity can be used according to the type of behavior to be modeled.

In large-scale network simulations, where many thousands of neurons and synapses must be simulated, it is clear that the simplest representation for voltage-dependent and synaptic currents is needed for reasons of computational efficiency. Integrate-and-fire models with simplified synaptic couplings are classically used in neural networks (reviewed in Arbib, 1995). However, electrophysiological experiments show that, in most regions of the brain, neurons exhibit complex intrinsic firing properties (Llinás, 1988) and possess multiple types of synaptic receptors (McCormick, 1992). In the example of thalamic oscillations, simplified schemes for synaptic interactions and Hodgkin-Huxley models of voltage-dependent currents provided acceptable representations to model network behavior as observed experimentally (see Section 7).

This approach therefore lays in-between the biophysical accuracy of multistate Markov schemes, derived from single-channel recordings, and highly simplified integrate-and-fire representations, commonly used in neural networks. Computational models allow us to explore the dynamic possibilities of neurons possessing multiple voltage-dependent currents and synaptic receptor types. Using simplified models of ionic currents will become increasingly useful to explore these complex systems, as new ion channel and receptor subtypes are identified, and as new interactions with cellular biochemistry are discovered.

8.3 Integration with molecular biology

Modeling membrane excitability, synaptic transmission and second-messenger actions using similar equations provides a full description of all electrical neuronal interactions using the same formalism (Destexhe et al., 1994c). Besides its aesthetic advantage, this approach is also useful because it uses a language that is compatible with molecular and biochemical descriptions. It

is therefore a natural description to adopt in order to link electrical activity to biochemistry, which is likely to become of increasing interest in the future.

A wide range of biological phenomena can be addressed by models that consider ion channels in a molecular and biochemical context as well as an electrical one. As a prominent example, the action of second-messengers such as G-proteins was considered here in the context of GABA_B receptors. G-proteins may not only act on ion channels, but may also affect various biochemical pathways, through adenylate cyclase, protein kinases, phospholipase C and gene regulation (Berridge and Irvine, 1989; Nelson and Alkon, 1991; Tang and Gilman, 1991; Birnbaumer, 1992; Clapham and Neer, 1993; Gutkind, 1998; Selbie and Hill, 1998). It is clear that when the action of synaptic receptors with biochemical pathways will be clarified, it will uncover a new dimension of complexity in neuronal interactions. It is likely to become increasingly difficult to understand the long-term behavior of neuronal networks intuitively, and computational models should play important role in helping us to understand these complex interactions.

Appropriate models are therefore needed to integrate electrophysiological knowledge with the intricate web of second-messengers, protein phosphorylation systems, and the deeper machinery of signal transduction and gene regulation. Kinetic models provide a natural way of integrating electrophysiology with cellular biochemistry, in which ion channels are considered as a special and important class of enzymes rather than as a completely distinct subject. Kinetic models of interactions through second-messengers and G-proteins mark only the initial stages of this integration.

References

- [1] Aldrich RW, Corey DP and Stevens CF (1983) A reinterpretation of mammalian sodium channel gating based on single channel recording. *Nature* **306**: 436-441.
- [2] Aldrich RW and Stevens CF (1987) Voltage-dependent gating of single sodium channels from mammalian neuroblastoma cells. *J. Neurosci.* **7**: 418-431.
- [3] Andersen O and Koeppe RE II (1992) Molecular determinants of channel function. *Physiol. Rev.* **72**: S89-S158.
- [4] Andersen P and Rutjord T (1964) Simulation of a neuronal network operating rhythmically through recurrent inhibition. *Nature* **204**: 289-190.
- [5] Andrade R, Malenka RC and Nicoll RA (1986) A G protein couples serotonin and GABA_B receptors to the same channels in hippocampus. *Science* **234**: 1261-1265.
- [6] Arbib M (Editor) (1995) *The Handbook of Brain Theory and Neural Networks*. MIT Press, Cambridge, MA.
- [7] Armstrong CM (1969) Inactivation of the potassium conductance and related phenomena caused by quaternary ammonium ion injection in squid axons. *J. Gen. Physiol.* **54**: 553-575.
- [8] Armstrong CM (1981) Sodium channels and gating currents. *Physiol. Rev.* **62**: 644-683.
- [9] Armstrong CM and Hille B (1998) Voltage-gated ion channels and electrical excitability. *Neuron* **20**: 371-380.
- [10] Augustine GJ and Charlton MP (1986) Calcium dependence of presynaptic calcium current and post-synaptic response at the squid giant synapse. *J. Physiol.* **381**:619-640.
- [11] Bartol TM Jr, Land BR, Salpeter EE and Salpeter MM (1991) Monte Carlo simulation of miniature endplate current generation in the vertebrate neuromuscular junction. *Biophys. J.* **59**: 1290-1307.
- [12] Berridge MJ and Irvine RF (1989) Inositol phosphates and cell signalling. *Nature* **341**: 197-205.
- [13] Bezanilla F (1985) Gating of sodium and potassium channels. *J. Membr. Biol.* **88**: 97-111.

- [14] Birnbaumer L (1992) Receptor-to-effector signaling through G proteins: roles for beta gamma dimers as well as alpha subunits. *Cell* **71**: 1069-1072.
- [15] Blaustein MP (1988) Calcium transport and buffering in neurons. *Trends Neurosci.* **11**: 438-443.
- [16] Borg-Graham LJ (1991) Modeling the nonlinear conductances of excitable membranes. In: Wheal H and Chad J, eds. *Cellular and Molecular Neurobiology: A Practical Approach*. Oxford University Press, New York. pp. 247-275.
- [17] Breitwieser GE and Szabo G (1988) Mechanism of muscarinic receptor-induced K⁺ channel activation as revealed by hydrolysis-resistant GTP analogues. *J. Gen. Physiol.* **91**: 469-493.
- [18] Brown DA (1990) G-proteins and potassium currents in neurons. *Annu. Rev. Physiol.* **52**: 215-242.
- [19] Brown AM and Birnbaumer L (1990) Ionic channels and their regulation by G protein subunits. *Annu. Rev. Physiol.* **52**: 197-213.
- [20] Bush P and Sejnowski TJ (1991) Simulations of a reconstructed cerebellar Purkinje cell based on simplified channel kinetics. *Neural Computation* **3**: 321-332.
- [21] Chabala LD (1984) The kinetics of recovery and development of potassium channel inactivation in perfused squid giant axons. *J. Physiol.* **356**: 193-220.
- [22] Chen C and Hess P (1990) Mechanisms of gating of T-type calcium channels. *J. Gen. Physiol.* **96**: 603-630.
- [23] Clapham, DE and Neer EJ (1993) New roles for G-protein $\beta\gamma$ -dimers in transmembrane signalling. *Nature* **365**: 403-406.
- [24] Clay JR (1989) Slow inactivation and reactivation of the potassium channel in squid axons. *Biophys. J.* **55**: 407-414.
- [25] Clements JD, Lester RAJ, Tong J, Jahr C, and Westbrook GL (1992) The time course of glutamate in the synaptic cleft. *Science* **258**: 1498-1501.
- [26] Clements JD (1996) Transmitter time course in the synaptic cleft: its role into central synaptic function. *Trends Neurosci.* **19**: 163-171.
- [27] Colquhoun D and Hawkes AG (1977) Relaxation and fluctuations of membrane currents that flow through drug-operated channels. *Proc. Roy. Soc. Lond. Ser. B* **199**: 231-262.
- [28] Colquhoun D and Hawkes AG (1981) On the stochastic properties of single ion channels. *Proc. Roy. Soc. Lond. Ser. B* **211**: 205-235.
- [29] Colquhoun D, Jonas P and Sakmann B (1992) Action of brief pulses of glutamate on AMPA/kainate receptors in patches from different neurons of rat hippocampal slices. *J. Physiol.* **458**, 261-287.
- [30] Contreras D, Destexhe A, Sejnowski TJ and Steriade M (1996) Control of spatiotemporal coherence of a thalamic oscillation by corticothalamic feedback. *Science* **274**: 771-774.
- [31] Contreras D, Destexhe A, Sejnowski TJ and Steriade M (1997) Spatiotemporal patterns of spindle oscillations in cortex and thalamus. *J. Neurosci.* **17**: 1179-1196.
- [32] Destexhe A and Sejnowski TJ (1995) G-protein activation kinetics and spill-over of GABA may account for differences between inhibitory responses in the hippocampus and thalamus. *Proc. Natl. Acad. Sci. USA* **92**: 9515-9519.
- [33] Destexhe A and Sejnowski TJ (1997) Synchronized oscillations in thalamic networks: insights from modeling studies. In: *Thalamus* (Steriade M, Jones EG, McCormick DA, ed), pp. 331-371. Amsterdam: Elsevier.
- [34] Destexhe A, Babloyantz A and Sejnowski TJ (1993a) Ionic mechanisms for intrinsic slow oscillations in thalamic relay neurons. *Biophys. J.* **65**: 1538-1552.
- [35] Destexhe A, Bal T, McCormick DA and Sejnowski TJ (1996a) Ionic mechanisms underlying synchronized oscillations and propagating waves in a model of ferret thalamic slices. *J. Neurophysiol.* **76**: 2049-2070.
- [36] Destexhe A, Contreras D and Steriade M (1998a) Mechanisms underlying the synchronizing action of corticothalamic feedback through inhibition of thalamic relay cells. *J. Neurophysiol.* **79**: 999-1016.
- [37] Destexhe A, Contreras D, Sejnowski TJ and Steriade M. (1994a) Modeling the control of reticular thalamic oscillations by neuromodulators. *NeuroReport* **5**: 2217-2220.
- [38] Destexhe A, Contreras D, Steriade M, Sejnowski TJ and Huguenard JR (1996b) In vivo, in vitro and computational analysis of dendritic calcium currents in thalamic reticular neurons. *J. Neurosci.* **16**: 169-185.

- [39] Destexhe A, Mainen Z and Sejnowski TJ (1994b) An efficient method for computing synaptic conductances based on a kinetic model of receptor binding. *Neural Computation* **6**: 14-18.
- [40] Destexhe A, Mainen ZF and Sejnowski TJ (1994c) Synthesis of models for excitable membranes, synaptic transmission and neuromodulation using a common kinetic formalism. *J. Computational Neuroscience* **1**: 195-230.
- [41] Destexhe A, Mainen ZF and Sejnowski TJ (1998b) Kinetic models of synaptic transmission. In: *Methods in Neuronal Modeling* (2nd edition) (ed. Koch C and Segev I), pp. 1-26. MIT Press, Cambridge, MA.
- [42] Destexhe A, McCormick DA and Sejnowski TJ (1993b) A model of 8-10 Hz spindling in interconnected thalamic relay and reticularis neurons. *Biophys. J.* **65**: 2474-2478.
- [43] Dutar P and Nicoll RA (1988) A physiological role for GABA_B receptors in the central nervous system. *Nature* **332**: 156-158.
- [44] Fitzhugh R (1965) A kinetic model of the conductance changes in nerve membrane. *J. Cell. Comp. Physiol.* **66**: 111-118.
- [45] Golomb D, Wang XJ and Rinzel J (1996) Propagation of spindle waves in a thalamic slice model. *J. Neurophysiol.* **75**: 750-769.
- [46] Gutkind JS (1998) The pathways connecting G protein-coupled receptors to the nucleus through divergent mitogen-activated protein kinase cascades. *J. Biol. Chem.* **273**: 1839-1842.
- [47] Harris AL, Spray DC and Bennett MVL (1981) Kinetic properties of a voltage-dependent junctional conductance. *J. Gen. Physiol.* **77**: 95-117.
- [48] Hestrin S (1992) Activation and desensitization of glutamate-activated channels mediating fast excitatory synaptic currents in the visual cortex. *Neuron* **9**: 991-999.
- [49] Hille B (1992) *Ionic Channels of Excitable Membranes*. Sinauer Associates INC, Sunderland, MA.
- [50] Hodgkin AL and Huxley AF (1952) A quantitative description of membrane current and its application to conduction and excitation in nerve. *J. Physiol.* **117**: 500-544.
- [51] Horn RJ, Patlak J and Stevens CF (1981) Sodium channels need not open before they inactivate. *Nature* **291**: 426-427.
- [52] Johnson FH, Eyring H and Stover BJ (1974) *The theory of rate processes in biology and medicine*, New York: John Wiley and Sons.
- [53] Jonas P, Major G and Sakmann B (1993) Quantal components of unitary EPSCs at the mossy fibre synapse on CA3 pyramidal cells of rat hippocampus. *J. Physiol.* **472**: 615-663.
- [54] Jones EG (1985) *The Thalamus*. Plenum Press, New York.
- [55] Keller BU, Hartshorne RP, Talvenheimo JA, Catterall WA and Montal M (1986) Sodium channels in planar lipid bilayers. Channel gating kinetics of purified sodium channels modified by batrachotoxin. *J. Gen. Physiol.* **88**:1-23.
- [56] Kim U, Bal T and McCormick DA (1995) Spindle waves are propagating synchronized oscillations in the ferret LGNd in vitro. *J. Neurophysiol.* **74**: 1301-1323.
- [57] Kim U, Sanches-Vives MV and McCormick DA (1997) Functional dynamics of GABAergic inhibition in the thalamus. *Science* **278**: 130-134.
- [58] Koch C and Segev I (Editors) (1998) *Methods in Neuronal Modeling* (2nd edition). MIT Press, Cambridge, MA.
- [59] Labarca P, Rice JA, Fredkin DR and Montal M (1985) Kinetic analysis of channel gating. Application to the cholinergic receptor channel and the chloride channel from *Torpedo Californica*. *Biophys. J.* **47**: 469-478.
- [60] Lamb TD and Pugh EN (1992) A quantitative account of the activation steps involved in phototransduction in amphibian photoreceptors. *J. Physiol.* **449**: 719-758.
- [61] Lester RA and Jahr CE (1992) NMDA channel behavior depends on agonist affinity. *J. Neurosci.* **12**: 635-643.
- [62] Levitt DG (1989) Continuum model of voltage-dependent gating. *Biophys. J.* **55**: 489-498.
- [63] Liebovitch LS and Sullivan JM (1987) Fractal analysis of a voltage-dependent potassium channel from cultured mouse hippocampal neurons. *Biophys. J.* **52**: 979-988.

- [64] Liebovitch LS and Toth TI (1991) A model of ion channel kinetics using deterministic chaotic rather than stochastic processes. *J. Theor. Biol.* **148**: 243-267.
- [65] Llinás RR (1988) The intrinsic electrophysiological properties of mammalian neurons: a new insight into CNS function. *Science* **242**: 1654-1664.
- [66] Magleby KL and Stevens CF (1972) A quantitative description of end-plate currents. *J. Physiol.* **223**: 173-197.
- [67] Marom, S and Abbott LF (1994) Modeling state-dependent inactivation of membrane currents. *Biophys. J.* **67**: 515-520.
- [68] McCormick DA (1992) Neurotransmitter actions in the thalamus and cerebral cortex and their role in neuromodulation of thalamocortical activity. *Progr. Neurobiol.* **39**: 337-388.
- [69] McCormick DA and Huguenard JR (1992) A model of the electrophysiological properties of thalamocortical relay neurons. *J. Neurophysiol.* **68**: 1384-1400.
- [70] McManus OB, Weiss DS, Spivak CE, Blatz AL and Magleby KL (1988) Fractal models are inadequate for the kinetics of four different ion channels *Biophys. J.* **54**: 859-870.
- [71] Millhauser GL, Saltpeper EE and Oswald RE (1988) Diffusion models of ion-channel gating and the origin of power-law distributions from single-channel recording. *Proc. Natl. Acad. Sci. USA* **85**: 1503-1507.
- [72] Neher E (1998) Vesicle pools and Ca^{2+} microdomains: new tools for understanding their role in neurotransmitter release. *Neuron* **20**: 389-399.
- [73] Neher E and Sakmann B (1976) Single-channel currents recorded from membrane of denervated muscle frog fibers. *Nature* **260**: 799-802.
- [74] Neher E and Stevens CF (1979) Voltage-driven conformational changes in intrinsic membrane proteins. In: FO Schmitt and FG Worden, eds. *The neurosciences. Fourth study program*, MIT Press, Cambridge, MA, pp. 623-629.
- [75] Nelson TJ and Alkon DL (1991) GTP-binding proteins and potassium channels involved in synaptic plasticity and learning. *Molec. Neurobiol.* **5**: 315-328.
- [76] Otis TS and Mody I (1992) Modulation of decay kinetics and frequency of GABA_A receptor-mediated spontaneous inhibitory postsynaptic currents in hippocampal neurons. *Neurosci.* **49**: 13-32.
- [77] Otis TS, Dekoninck Y and Mody I (1993) Characterization of synaptically elicited GABA_B responses using patch-clamp recordings in rat hippocampal slices. *J. Physiol.* **463**: 391-407.
- [78] Patneau DK and Mayer ML (1991) Kinetic analysis of interactions between kainate and AMPA: evidence for activation of a single receptor in mouse hippocampal neurons. *Neuron* **6**: 785-798.
- [79] Perozo E and Bezanilla F (1990) Phosphorylation affects voltage gating of the delayed rectifier K⁺ channel by electrostatic interactions. *Neuron* **5**: 685-690.
- [80] Rall W (1967) Distinguishing theoretical synaptic potentials computed for different soma-dendritic distributions of synaptic inputs. *J. Neurophysiol.* **30**, 1138-1168.
- [81] Rall W (1995) *The Theoretical Foundation of Dendritic Function* (Segev I, Rinzel J, Shepherd GM, ed). Cambridge: MIT Press.
- [82] Raman IM and Trussell LO (1992) The kinetics of the response to glutamate and kainate in neurons of the avian cochlear nucleus. *Neuron* **9**:173-186.
- [83] Sakmann B and Neher E (Editors) (1995) *Single-Channel Recording* (2nd edition). Plenum Press, New York, NY.
- [84] Sansom MSP, Ball FG, Kerry CJ, Ramsey RL and Usherwood PNR (1989) Markov, fractal, diffusion, and related models of ion channel gating. A comparison with experimental data from two ion channels. *Biophys. J.* **56**: 1229-1243.
- [85] Selbie LA and Hill SJ (1998) G protein-coupled-receptor cross-talk: the fine-tuning of multiple receptor-signalling pathways. *Trends Pharmacol. Sci.* **19**: 87-93.
- [86] Sigworth FJ and Neher E (1980) Single Na channel currents observed in cultured rat muscle cells. *Nature* **287**: 447-449.
- [87] Standley C, Ramsey RL and Usherwood PNR (1993) Gating kinetics of the quisqualate-sensitive glutamate receptor of locust muscle studied using agonist concentration jumps and computer simulations. *Biophys. J.* **65**: 1379-1386.

- [88] Steriade M and Llinás RR (1988) The functional states of the thalamus and the associated neuronal interplay. *Physiol. Reviews* **68**: 649-742.
- [89] Steriade M, McCormick DA and Sejnowski TJ (1993) Thalamocortical oscillations in the sleeping and aroused brain. *Science* **262**: 679-685.
- [90] Stevens CF (1978) Interactions between intrinsic membrane protein and electric field. *Biophys. J.* **22**: 295-306.
- [91] Szabo G and Otero AS (1989) Muscarinic activation of potassium channels in cardiac myocytes: kinetic aspects of G protein function in vivo. *Trends Pharmacol. Sci.* Dec. 1989 Suppl.: 46-49.
- [92] Tang MJ and Gilman AG (1991) Type-specific regulation of adenylyl cyclase by G protein beta gamma subunits. *Science* **254**: 1500-1503.
- [93] Thalmann RH (1988) Evidence that guanosine triphosphate (GTP)-binding proteins control a synaptic response in brain: effect of pertussis toxin and GTP gamma S on the late inhibitory postsynaptic potential of hippocampal CA3 neurons. *J. Neurosci.* **8**: 4589-4602.
- [94] Thompson SM and Gähwiler BH (1992) Effects of the GABA uptake inhibitor tiagabine on inhibitory synaptic potentials in rat hippocampal slice cultures. *J. Neurophysiol.* **67**: 1698-1701.
- [95] Vandenberg CA and Bezanilla F (1991) A model of sodium channel gating based on single channel, macroscopic ionic, and gating currents in the squid giant axon. *Biophys. J.* **60**: 1511-1533.
- [96] VanDongen AMJ, Codina J, Olate J, Mattera R, Joho R, Birnbaumer L and Brown AM (1988) Newly identified brain potassium channels gated by the guanine nucleotide binding protein G_o . *Science* **242**: 1433-1437.
- [97] von Krosigk M, Bal T and McCormick, DA (1993) Cellular mechanisms of a synchronized oscillation in the thalamus. *Science* **261**: 361-364.
- [98] Walaas SI and Greengard P (1991) Protein phosphorylation and neuronal function. *Pharmacol. Rev.* **43**: 299-349.
- [99] Wang XJ and Rinzel J (1992) Alternating and synchronous rhythms in reciprocally inhibitory model neurons. *Neural Computation* **4**: 84-97.
- [100] Wang XJ, Golomb D and Rinzel J (1995) Emergent spindle oscillations and intermittent burst firing in a thalamic model: specific neuronal mechanisms. *Proc. Natl. Acad. Sci. USA* **92**: 5577-5581.
- [101] Yamada WM and Zucker RS (1992) Time course of transmitter release calculated from simulations of a calcium diffusion model. *Biophys. J.* **61**: 671-682.
- [102] Yamada WN, Koch C and Adams PR (1989) Multiple channels and calcium dynamics. In C Koch and I Segev, eds., *Methods in Neuronal Modeling*. Cambridge, MA: MIT Press, pp. 97-134.